Journal of Applied Fluid Mechanics, Vol. x, No. x, pp. x-x, 200x.
Available online at www.jafmonline.net, ISSN 1735-3645, EISSN 1735-3645.

Analysis and Prediction of Equivalent Diameter of Air Bubbles Rising in Water

L. B. Calazan[1†], M. S. Andrade[2], F. P. de Moura[3] and G. de C. Nascimento[4]

[1.] *Engineering School, Fluminense Federal University, Niterói 24210-240, Rio de Janeiro, Brazil*
[2.] *Engineering School, Fluminense Federal University, Niterói 24210-240, Rio de Janeiro, Brazil*
[3.] *Institute of Chemistry, Fluminense Federal University, Niterói 24210-240, Rio de Janeiro, Brazil*
[4.] *Department of Agricultural and Environmental Engineering, Fluminense Federal University, Niterói 24210-240, Rio de Janeiro, Brazil*

†*Corresponding Author Email: contatolorenabc@gmail.com*

ABSTRACT

The equivalent diameter of rising bubbles in liquids is an important parameter studied for decades by researchers, with different types of purposes. In the analysis of submarine leaks, aiming to reduce their negative effects, this parameter serves as the groundwork for critical points of the scenario, such as flow rate and terminal velocity. Most of the literature on the subject is related to the study of air bubbles in water, being, therefore, the main guide of the experimental apparatus of this article. After 21 tests with air bubble chain in tap water, varying the flow rate (between 21.1mL / min and 234.4mL / min) and using different orifice leakage inner diameters (1mm, 2mm and 5mm), comparisons were made with works of the main authors in the field. The equivalent diameters of bubbles varied from 4.1mm to 8.2mm, being compatible with those found in the literature. The results were successful for validation of the experimental method, in other to serve as a basis for future analyzes directed to other parameters of the system.

Keywords: bubble equivalent diameter, orifice inner diameter, flow rate, bubble volume, fluid.

NOMENCLATURE

Bd	Bond number	*Q*	flow rate
d_e	equivalent diameter	*Ra*	Ratio of liquid and gas viscosity
d_o	capillary inner diameter	*Re*	Reynolds number
Eo	Eotvos number	*t*	time
f	factor of correction	*u*	velocity
fe	frequency of bubble emission	u_o	orifice superficial velocity
Fr	Froude number	V_{air}	air volume
g	gravity acceleration	V_b	bubble volume
Ga	Galileo number	*w*	largest dimension of bubble
h	perpendicular dimension of *w*	μ	viscosity
L	inferior length of bubble	ρ	density
n_b	number of bubbles counted	σ	interfacial tension
Subscripts			
1	major segment	*l*	liquid
2	minor segment	*g*	gas

1. INTRODUCTION

Several industrial processes are based on multiphase systems of bubbles rising in liquids, in fields related to chemistry, petro chemistry, biochemistry and metallurgic (Chen, 2005). This system is applied in process as aeration, flotation, fermentation control, microbiological growth, gasification, reagents addition, catalysis, and induced agitation (Moys et al., 2010; Yang et al., 2016; Behr; Becker and Dostal., 2009). Its use is due to excellent mixing, momentum, mass and heat transfer characteristics (Huang et al., 2017; Behr; Becker and Dostal., 2009; Krishna and Van Baten, 2003; Gupta et al., 2001). In addition to industrial processes another important system is leakage of gas in subsea wells and pipelines, which represent high financial and environmental costs.

Many authors studied the rising bubble volume and parameters that affect. For this type of study, usually is adopted the concept of equivalent diameter, which is defined as the diameter equivalent to a perfect sphere diameter of equal volume, given by the following equation:

$$V_b = \frac{\pi d_e^3}{6} \quad (1)$$

where d_e is the equivalent diameter and V_b is the bubble volume.

The first substantial progress in predicting bubble volume was obtained in 1864, through the relationship between the specific mass differential ($\Delta\rho = \rho_l - \rho_g$), the gravity acceleration (g), the capillary inner diameter (d_o) and the interfacial tension of both fluids (σ). A traction factor was also used for correction of contact angles other than 90° (Tate, 1864).

Tate justified his work based on medical prescriptions for non-standardized drops of medicines. The work reached drops of liquids, but was widely used for gas bubbles. However, this approach is used for quasi-static conditions, with extremely low flow rate situations (Shi, 2012).

Many authors have developed equations to predict the equivalent diameter of bubbles and drops, applied to both different scenarios and fluid properties. The main equations available in the literature were selected and divided into those that consider the flow rate (Q) and those that use dimensionless parameters.

As seen in Table 1.a, the flow rate sometimes appears as a single parameter in equations for calculating the equivalent diameter, being only necessary to adjust the range of the different physical properties of fluids to the apply scenario of each one. The orifice superficial velocity (u_o) is the ratio between the flow rate and the orifice inner area, therefore, it is an alternative parameter for flow rate analysis.

Dimensional parameters, both those consolidated in the literature and those proposed by the authors themselves, are commonly used to calculate the bubble equivalent diameter. In general, they are based on the properties of fluids, sometimes also linked to terminal velocity, as shown in Table 1.b.

To study the bubble formation, shape, aspect ratio and equivalent diameter, as well as their velocity, usually, experimental systems are prepared in the laboratory (Haberman and Morton, 1953; Marks, 1973; Wu, 2002; Tomiyama, 2002; Shew, 2006; Melo, 2007; Liu, 2014; Sharaf, 2017; Wang and Socolofsky, 2015). In general, the experiments consist of a tank filled with a working liquid, an injection orifice at the bottom, an injection system and a camera.

X and Y tank dimensions are sufficiently high to be an infinite walls problem, without walls interference. The Z dimension is varied and depends on the technique and parameters that will be used in the experiment. In literature it varies from 30 (Liu, 2015) to 200 cm (Shew, 2006).

The injection system is mostly performed by syringes (Liu, Yan and Zhao, 2015; Sharaf *et al.*, 2017; Tomiyama *et al.*, 2002; Wu and Gharib, 2002) or cylinders (Haberman and Morton, 1953; Marks, 1973; Wang and Socolofsky, 2015). In some cases, there is a bulkhead above the outlet of the orifice, aiming at the production of larger bubbles (Haberman and Morton, 1953; Marks, 1973; Raymond and Rosant, 2000). As shown in Table 2, the range of both orifice inner diameter and experimental bubble equivalent diameter studied by the authors are of diversified magnitude.

One or more cameras are positioned to capture images of the fluid-fluid system, in photo and/or video format (Haberman and Morton, 1953; Liu, Yan and Zhao, 2015; Marks, 1973; Melo, 2007; Raymond and Rosant, 2000; Wu and Gharib, 2002; Xiao *et al.*, 2019; Sharaf *et al.*, 2017; Tomiyama *et al.*, 2002; Shew, 2006; Wang and Socolofsky, 2015). In order to improve the images, a light source behind the tank is frequently used to refine the sharpness of bubbles (Haberman and Morton, 1953; Liu, Yan and Zhao, 2015; Melo, 2007; Raymond and Rosant, 2000; Sharaf *et al.*, 2017; Wang and Socolofsky, 2015; Xiao *et al.*, 2019)

As seen in previous paragraphs, many authors performed experimental tests in order to analyze different parameters of air bubbles. However, only Wang and Socolofsky (2015) performed testes with chain air bubbles in tap water. Another similarity between the author and the present work was the performance of testes with different flow rate, presenting their range used as shown in Table 6. On the other hand, Wang and Socolofsky (2015) opted to use similar circumstances to seabed, although measures of pressure and temperature were not specified in the article. The work was, therefore, chosen as the best comparison of experimental methodology in the literature, able to provide relevant data and information about subsea environment simulations.

2. EXPERIMENTAL APPARATUS AND PROCEDURES

The experimental apparatus used is represented

schematically by Fig. 1. A glass tank was filled with tap water at room temperature and pressure (25 °C and 1 atm). The height of the tank was 400 mm, with a rectangular cross section of 400 x 600 mm, enough to neglect the wall effects.

The gas injection system consisted of an air compressor, a cylinder and a rigid plastic tube, connected to the tank through a hole in the side. The cylinder function was to stabilize any intermittence in the air flow. A total of 21 tests were performed, varying the orifice inner diameter between 1, 2 and 5 mm. All took place in the bubbles chain regime, with flow rate variation, as shown in Fig. 2. The voltage regulator allowed the variation of the flow rate, connected to the injection system by a voltage stabilizer.

The test videos had a duration ranging from 6 to 10s and were obtained at a rate of 240 frames per second (fps), which resulted in a wide variety of bubbles per test. The camera used was the Xiaomi Mi 9t phone, with 1280 x 720 pixels in one frame. A light source was positioned above the tank with two bulkheads, creating a slit of light on the bubble axis. This made the bubbles sharper and decrease the reflection of light. The background of the tank was internally opaque, preventing the appearance of shadows from bubbles. A scale with gradation at the millimeter level was positioned parallel to the vertical axis of bubbles, serving as a reference for the videos. The experimental system could be seen in Fig. 3.

The air leaked volume (V_{air}) was measured through a beaker, positioned inside the tank, with the opening facing downwards, so that it was possible to collect air bubbles. The time interval (Δt) was measured using a chronometer. Three volume and time measurements were made in each test.

To determine the flow rate (Q) of the tests, the direct method was applied, in other words, the ratio between the air leaked volume (V_{air}) and the time interval (Δt) corresponding to the leak (Equation 2), as shown in the following equation:

$$Q = \frac{V_{air}}{\Delta t} \tag{2}$$

From the obtained videos, the number of air bubbles (n_b) was counted during a certain time interval (Δt_c) and the frequency of bubble emission (f_e) was calculated by the following equation:

$$f_e = \frac{n_b}{\Delta t_c} \tag{3}$$

The volume of a leaked air bubble (V_b) was obtained from the flow rate (Q) and the emission frequency (f_e), considering that bubbles have the same size, as shown in the following equation:

$$V_b = \frac{Q}{f_e} \tag{4}$$

Finally, the bubble equivalent diameter (d_e) was acquired from the sphere volume equation, as shown in the following equation:

$$d_e = \sqrt[3]{\frac{6 \times V_b}{\pi}} \tag{5}$$

Water and air specific gravity were measured using Digital Densimeter DMA 5000 (Anton-Paar) with syringe injection in closed system. Water viscosity was measured using a manual Cannon-Fenske Viscometer Tube (Sigma-Aldrich). Air viscosity and superficial tension for water and air were assumed from values enshrined in technical literature. The results are given by Table 3.

3. RESULTS AND DISCUSSION

The experimental results of flow rate and bubble equivalent diameter are presented with the respective orifice inner diameter in Table 4, as well as the number of tests performed in each case. Within each scenario, the 5 flow rate values were distributed proportionally between the minimum and maximum flows found, which were characterized respectively by the beginning of constant formation between bubbles and the moment immediately before the plume formation.

Wang and Socolofsky (2015) studied the motion of air bubbles that were continuously released from an orifice with diameter 4.0 mm into still water. Their experiment led to equivalent diameters in the range from 4.4 to 5.7 mm, by using frequency varied from 84 to 734 bubbles/min. Based on that, their experimental results were plotted together with those of the present work, as shown in Fig. 4. The analysis of Q versus d_e indicated a growth in the bubble equivalent diameter due to the increase in the orifice inner diameter. It is also noteworthy that the increased flow rate also contributed to higher values of bubble equivalent diameter.

It is remarkable how results from the present work are consistent when compared to author experimental tests, once linearity occurs in results as the orifice inner diameter increases. Furthermore, it is observed that the author's results, referring to d_o = 4 mm, are consistently among the results referring to d_o = 2mm and d_o = 5mm of the present work.

The greater proximity observed with d_o = 2mm can be justified by the distinct ambience used by the author, in similar circumstances to seabed. In relation to the fluid properties, as shown in table 3, the values indicate a possible system at a temperature lower than the room temperature used in the present work. In addition, it is possible that the author performed their tests in a higher pressure environment, contributing to obtaining smaller values for equivalent bubble diameter.

The results obtained by the bubble equivalent diameter were also compared with values calculated through equations made by other authors, using the fluid properties, experimental flow rate and orifice inner diameter of the present work. The average percentage between each calculated d_e and the respective experimental value found in this work were presented by author, as shown in Table 5.

Regarding the equations of previosly referenced authors, it is remarkable that Akita and Yoshida

(1974), Jamialahmadi (2001) and Gaddis and Voeglepohl (1986) have more agreement with this work results. Thus, these authors were chosed to be compared with this present work along all bubbles diameters obtained in the 21 cases studied. The comparasion was ploted in Fig. 5, where is possible to observe that the deviation of predictions are mostly closed to the results obtained (up to ±25%).

The experimental results were also plotted against the equations of the three selected authors, separated by orifice inner diameter, based on their respective equations. The best convergence obtained was at the d_o = 1 mm, with all equations analyzed, as shown in Fig. 6.a.

The orifice inner diameter of 2 mm showed intermediate convergence, approaching more than two among the three authors (Jamialahmadi, 2001; Gaddis and Voeglepohl, 1986). It is remarkable that the experimental slope was the same as that of Gaddis and Vogelpohl (1986), as shown in Fig. 6.b. The orifice inner diameter of 5 mm, in turn, showed less compatibility among all of them, as shown in Fig. 6.c. Despite the distance, which can be explained by the instability inherent to large-diameter bubbles, the linearity similar to the main authors is notorious (Jamialahmadi, 2001; Gaddis and Voeglepohl, 1986).

The results were consistent with those observed in the literature. Akita and Yoshida (1974) show greater dispersion in the calculated results than Gaddis and Vogelpohl (1986) and Jamialahmadi (2001), which is the factor responsible for their greater distance from the experimental results, despite having a small average distance. In addition, it is important to emphasize that Gaddis and Vogelpohl (1986) and Jamialahmadi (2001), unlike Akita and Yoshida (1974), take into account the properties of fluids, thus having greater credibility for validating the results of the present work.

At last, Fig. 7 indicated the equations of the main authors and the experimental results from Wang and Socolofsky (2015), all calculated considering orifice inner diameter of 4 mm and both flow rate and fluid properties author's. The assumption that the author used a higher pressure value in his tests can be used again as a justification for the experimental data being slightly below the predictions of other authors. Despite this, it is possible to verify that the experimental data behave in a similar way to Gaddis and Vogelpohl (1986) and Jamialahmadi (2001), giving credibility to their results.

4. CONCLUSIONS

The experimental results showed growth of the bubble equivalent diameter with the increase of the orifice inner diameter. Preliminary analyzes have already showed an increase in bubble instability for larger equivalent diameters, a factor that may be linked to greater compatibility of results using the smaller d_o: 1 > 2 > 5 mm.

In this way, it is possible to highlight the theoretical and practical validation of the experiments performed against the equations of the authors Akita and Yoshida (1974), Gaddis and Voeglepohl (1986), Jamialahmadi (2001) and the experiments of Wang and Socolofsky (2015). When compared to the last one, it is important to emphasize that consists as the closest author in terms of results, considering the use of the same fluid-fluid system, even so with different environmental conditions.

In reference to the equations, the similarity of the experimental tests to authors' results differs due to the orifice inner diameter. Overall, the 5 mm orifice had the lowest compatibility of results, while the 1 mm orifice had the best convergence. Furthermore, the authors Jamialahmadi (2001) and Gaddis and Voeglepohl (1986) obtained greater agreement with the 2 mm orifice when compared to the rest of the authors, for considering the physical properties of fluids.

Finally, as possible future study fronts, extensive and detailed experiments with subsea temperature and pressure simulations are indicated. In addition, once the correlation between flow rate, orifice inner diameter and bubble equivalent diameter were evidenced, it is important to work on others relevant parameters such as terminal velocity and bubble trajectory.

REFERENCES

AKITA, K., and YOSHIDA, F. Bubble size, interfacial area, and liquid-phase mass transfer coefficient in bubble columns. **Industrial & Engineering Chemistry Process Design and Development**, 13(1), 84-91, 1974.

BEHR, Arno; BECKER, Marc; DOSTAL, Johannes. Bubble-size distributions and interfacial areas in a jetloop reactor for multiphase catalysis. **Chemical Engineering Science.** v. 64, n. 12, p. 2934-2940, 2009.

CHEN. P.; DUDUKOVIC. M. P.; SANYAL. J. Three-dimensional simulation of bubble column flows with bubble coalescence and breakup. **Aiche Journal**, v. 51, n. 3, p. 696-712, 2005.

DAVIDSON, J.F. and HARRISON, H. Fluidized particles. **Cambridge University Press**, Cambridge, UK, 1963.

DAVIDSON, J.F. and SCHULER, B.O. Bubble formation at an orifice in a viscous liquid. **Trans. Instn Chem**. Engrs, n. 38, p. 144-154, 1960.

GADDIS, E.s.; VOGELPOHL, A. Bubble formation in quiescent liquids under constant flow conditions. **Chemical Engineering Science.** v. 41, n. 1, p. 97-105, 1986.

GUPTA, Puneet; ONG, Booncheng; AL-DAHHAN, Muthanna H.; DUDUKOVIC, Milorad P.; TOSELAND, Bernard A. Hydrodynamics of churn turbulent bubble columns: gas⁝liquid recirculation and mechanistic modeling. **Catalysis Today.** v. 64, n. 3-4, p. 253-269, 2001.

HABERMAN. W. L.; MORTON. R. K. **An experimental investigation of the drag and shape of air bubbles rising in various liquids**. [S.l: s.n.],

1953.

HUANG, Jie; SAITO, Takayuki. Influences of gas–liquid interface contamination on bubble motions, bubble wakes, and instantaneous mass transfer. **Chemical Engineering Science.** v. 157, p. 182-199, 2017.

JAMIALAHMADI, M.; ZEHTABAN, M.R.; MÜLLER-STEINHAGEN, H.; SARRAFI, A.; SMITH, J.M. Study of Bubble Formation Under Constant Flow Conditions. **Chemical Engineering Research And Design.** v. 79, n. 5, p. 523-532, 2001.

KRISHNA, R.; VAN BATEN, J.M. Mass transfer in bubble columns. **Catalysis Today.** v. 79-80, p. 67-75, 2003.

KUMAR, R.; KULOOR, N.K. The Formation of Bubbles and Drops. **Advances In Chemical Engineering** Volume 8. p. 255-368, 1970.

LIU, Liu; YAN, Hongjie; ZHAO, Guojian. Experimental studies on the shape and motion of air bubbles in viscous liquids. **Experimental Thermal and Fluid Science** v. 62, p. 109–121, 2015.

MARKS, C. H. Measurements of the Terminal Velocity of Bubbles Rising in a Chain. **ASME Pap** n. 72- WA/FE-24, 1973.

MELO, Fabiana Regina Grandeaux. **Fluidodinâmica de esferas leves e bolhas em líquidos**. Programa de Pós-Graduação em Engenharia Química, Faculdade de Engenharia Química, Universidade Federal de Uberlândia, Uberlândia, 2007.

MIYAHARA, Toshiro; HAMAGUCHI, Masahiko; SUKEDA, Yoshiaki; TAKAHASHL, Teruo. Size of bubbles and liquid circulation in a bubble column with a draught tube and sieve plate. **The Canadian Journal Of Chemical Engineering**.v.64, n.5, p.718-725, 1986.

MOYS, M.H.; YIANATOS, J.; LARENAS, J. Measurement of particle loading on bubbles in the flotation process. **Minerals Engineering,** v. 23, n. 2, p. 131-136, 2010.

RAYMOND, F.; ROSANT, J. M. A numerical and experimental study of the terminal velocity and shape of bubbles in viscous liquids. **Chemical Engineering Science** v. 55, n. 5, p. 943–955, 2000.

SHARAF, D M *et al.* **Shapes and paths of an air bubble rising in quiescent liquids**. n. region IV, p. 1–13, 2017.

SHEW, Woodrow L.; PONCET, Sebastien; PINTON, Jean-François. Force measurements on rising bubbles. **Journal Of Fluid Mechanics**. v. 569, p. 51. Cambridge University Press, 2006.

SHI, S. Foundation Engineering of Coal Hydroliquefaction. **Chemical Industry Press**, Beijing, 2012.

TATE, T. On the magnitude of a drop of liquid formed under different circumstances. **The London, Edinburgh, And Dublin Philosophical Magazine And Journal Of Science**. v. 27, n. 181, p. 176-180, 1864.

TOMIYAMA, A. *et al.* Terminal velocity of single bubbles in surface tension force dominant regime. **International Journal of Multiphase Flow** v. 28, n. 9, p. 1497–1519, 2002.

VAN KREVELEN, D. W., and HOFTIJZER, P. J. (1950). Calculation of Interfacial Area in Bubble Contractors. **Chemical Engineering Progress**, n.46, p.29-35.

WANG, B. and SOCOLOFSKY, S.A. (2015) **On the Bubble Rise Velocity of a Continually Released Bubble Chain in Still Water and with Crossflow**. Physics of Fluids, 27, 103301-103321.

WU, Mingming; GHARIB, Morteza. Experimental studies on the shape and path of small air bubbles rising in clean water. **Physics of Fluids** v. 14, n. 7, 2002.

XIAO, Hang *et al.* Bubble formation in continuous liquid phase under industrial jetting conditions. **Chemical Engineering Science** v. 200, p. 214–224, 2019.

YANG, Zongbo; CHENG, Jun; LIN, Richen; ZHOU, Junhu; CEN, Kefa. Improving microalgal growth with reduced diameters of aeration bubbles and enhanced mass transfer of solution in an oscillating flow field. **Bioresource Technology**. v. 211, p. 429-434, 2016.

Table 1.a Equations for calculating d_e through Q.

Reference	Equation
Van Krevelen and Hoftijzer, 1950	$d_e = \left(1.722 \times \frac{6}{\pi} \times \frac{Q^{\frac{5}{6}}}{g^{\frac{3}{5}}}\right)^{\frac{1}{3}}$
Davidson and Schuler, 1960	$d_e = \left(1.378 \times \frac{6}{\pi} \times \frac{Q^{\frac{5}{6}}}{g^{\frac{3}{5}}}\right)^{\frac{1}{3}}$
Davidson and Harrison, 1963	$d_e = \left(1.138 \times \frac{6}{\pi} \times \frac{Q^{\frac{5}{6}}}{g^{\frac{3}{5}}}\right)^{\frac{1}{3}}$
Kumar and Kullor, 1967	$d_e = \left(0.976 \times \frac{6}{\pi} \times \frac{Q^{\frac{5}{6}}}{g^{\frac{3}{5}}}\right)^{\frac{1}{3}}$
Akita and Yoshida, 1974	$d_e = 1.88 \times d_o \times \left(\frac{u_o}{\sqrt{g \times d_o}}\right)^{\frac{1}{3}}$
Gaddis and Vogelpohl, 1986	$d_e = \left[\left(\frac{6 \times \sigma \times d_o}{\rho \times g}\right)^{\frac{4}{3}} + \left(\frac{81 \times Q \times \upsilon}{\pi \times g}\right) + \left(\frac{135 \times Q^2}{4 \times g \times \pi^2}\right)^{\frac{4}{5}}\right]^{\frac{1}{4}}$

Table 1.b Equations for calculating d_e through dimensionless parameters.

Author	Equation
Tate, 1864	$d_e = \left(\frac{f \times \pi \times \sigma \times d_o}{\Delta\rho \times g}\right)^{\frac{1}{3}}$
Jamialahmadi, 2001	$d_e = d_o \left[\frac{5}{Bd^{1.008}} + \left(\frac{9.26 Fr^{0.36}}{Ga^{0.39}}\right) + 2.147 \times Fr^{0.51}\right]^{\frac{1}{3}}$
Shi, 2012	$d_e = 1.82 \times \left(\frac{d_o}{Eo^{\frac{1}{3}}}\right)$
Xiao, 2019	$d_e = d_o \left(1.82 + \left(\frac{1.4773 Re_g Ra}{20691.2238 \left(Re_g Ra\right)^{0.05242} + \left(\frac{Ra Re_g}{Re_l}\right)^2}, 1.2815\right) + 0.02218 Re_l^{-0.4771} Re_g^{0.9952} Eo^{-0.0008095}\right) E$

Table 2 Range of d_o and experimental d_e of authors.

Author	d_e (mm)	d_o (mm)
Haberman and Morton (1953)	0.4 - 20	-
Marks (1973)	1.2 - 19	-
Tomiyama et al. (2002)	0.6 – 5.5	0.51, 0.9, 1.45 and 3.19
Wu and Gharib (2002)	1 -2	0.27 – 0.44
Shew et al. (2006)	1.74 – 2.4	0.3
Liu et al. (2015)	0.54 – 10.2	0.6 – 7.7
Sharaf et al. (2017)	1.4 – 26.7	0.6
Wang and Socolofsky (2015)	4.4 – 5.7	4.0

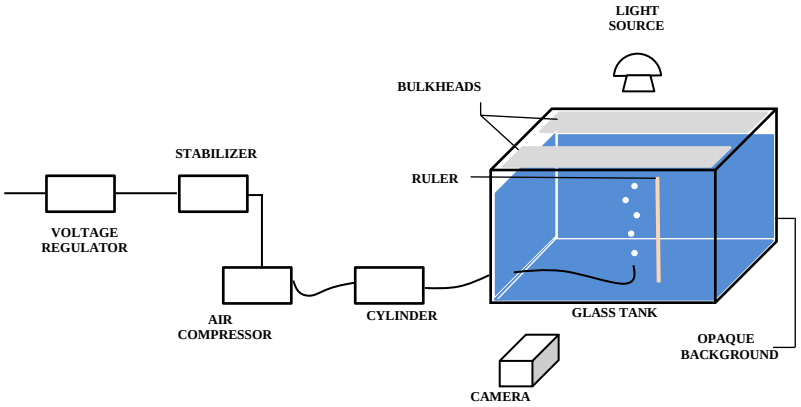

Fig. 1. Experimental schematic.

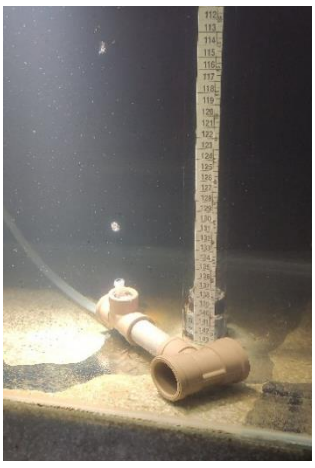

Fig. 2. Bubbles rising near the orifice (5 mm).

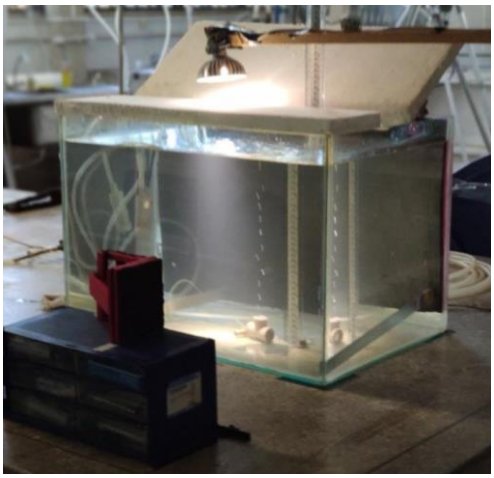

Fig. 3. Bubbles chain in tests tank and lightning system.

Table 3 Fluids properties.

Fluid	ρ (kg/m³)	μ (kg/m.s)	σ (N/m)
Water	998	1.02×10^{-3}	0.072
Air	1.20	1.72×10^{-5}	~0

Table 4 Relation of experimental results.

Orifice inner diameter	Number of tests performed	Q (mL/min)	d_e (mm)
1 mm	7	21.1 – 101.2	4.1 – 4.5
2 mm	7	25.2 – 153.2	4.8 – 5.9
5 mm	7	30.0 – 234.4	6.4 – 8.2

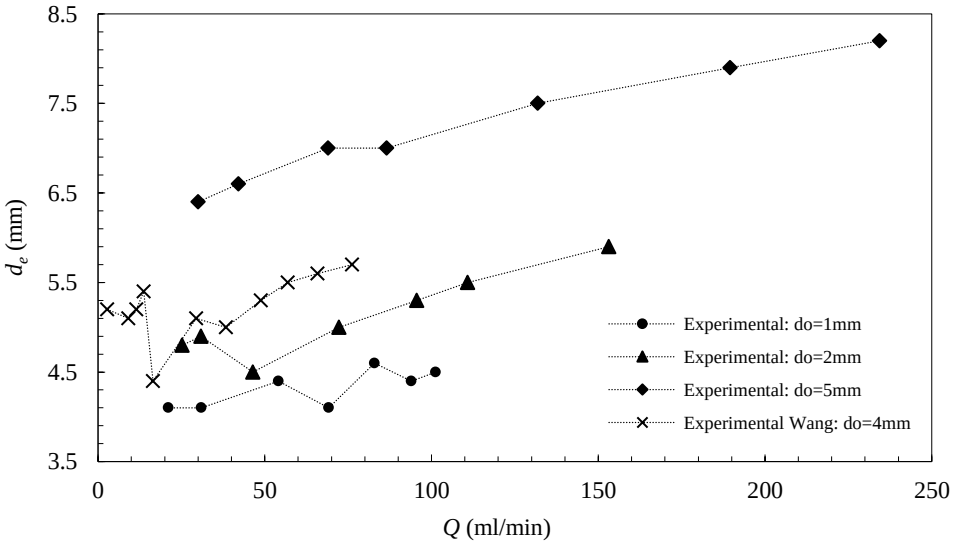

Fig. 4. Experimental d_e *versus* Q, for different d_o.

Table 5 Deviation between experimental d_e and authors' predictions.

Correlation	Percent average error (trust rating = 95%)
Van Krevelen and Hoftjizer (1950)	-25 ± 7.9
Davidson and Schuler (1960)	-30 ± 7.3
Kumar and Kuloor (1967)	-38 ± 6.5
Akita and Yoshida (1974)	-2.2 ± 6.8
Gaddis and Vogelpohl (1986)	-7.0 ± 2.4
Miyahara (1986)	33 ± 5.6
Jamialahmadi (2001)	-4.5 ± 2.4
Shi (2012)	-15 ± 3.1
Xiao (2019)	86 ± 12

Table 6 Experimental results from Wang and Socolofsky (d_o = 4mm)

Experimental test	Q (mL/min)	d_e (mm)
1	2.8	5.2
2	9.1	5.1
3	11.5	5.2
4	13.7	5.4
5	16.5	4.4
6	29.4	5.1
7	38.4	5.0
8	48.8	5.3
9	56.9	5.5
10	65.8	5.6
11	76.2	5.7

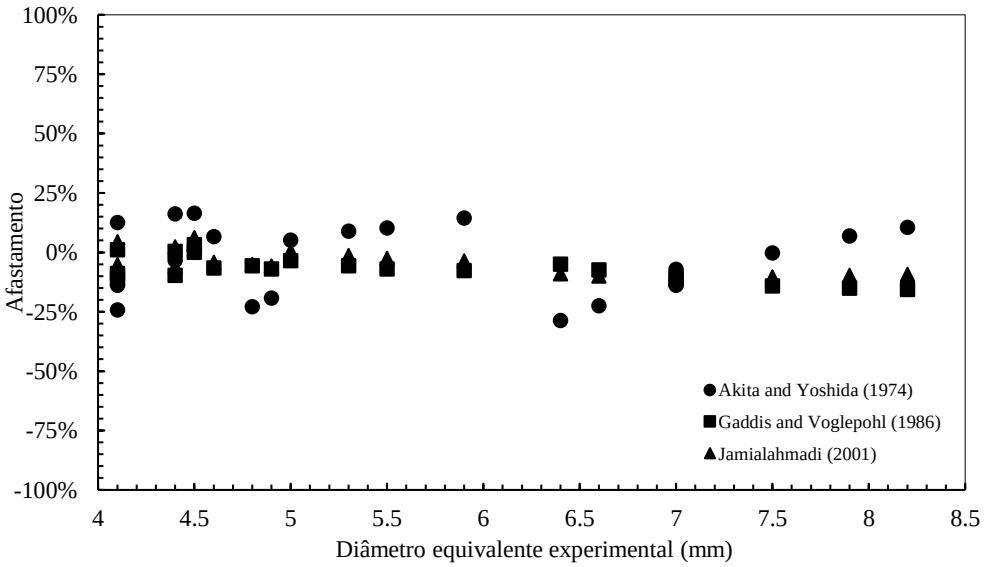

Fig. 5. Deviation between calculated d_e of the main authors and experimental d_e.

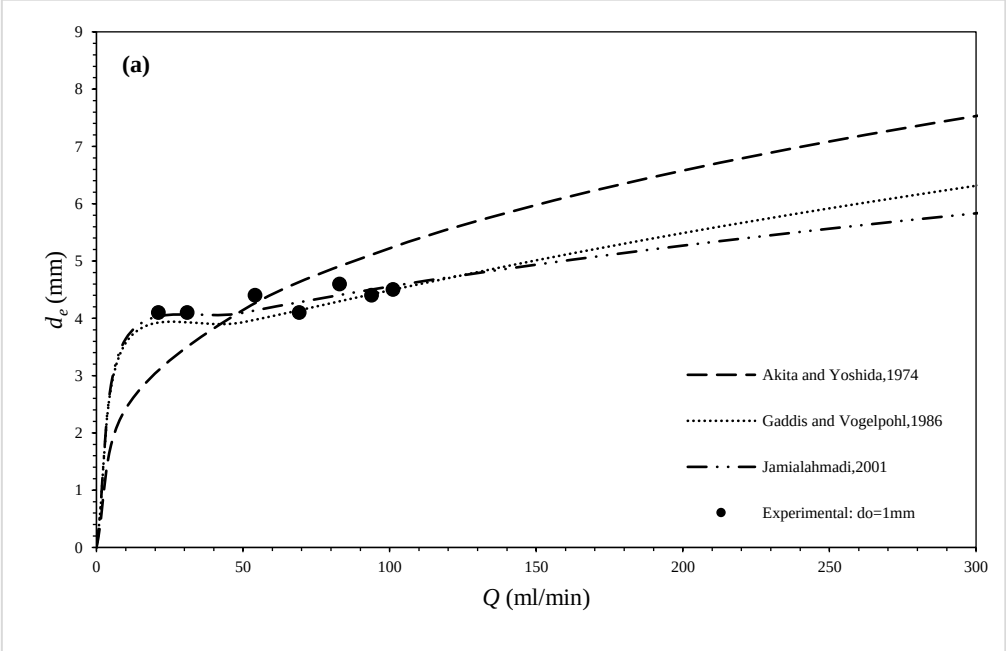
(a)
d_e (mm)
Q (ml/min)
Akita and Yoshida,1974
Gaddis and Vogelpohl,1986
Jamialahmadi,2001
Experimental: do=1mm

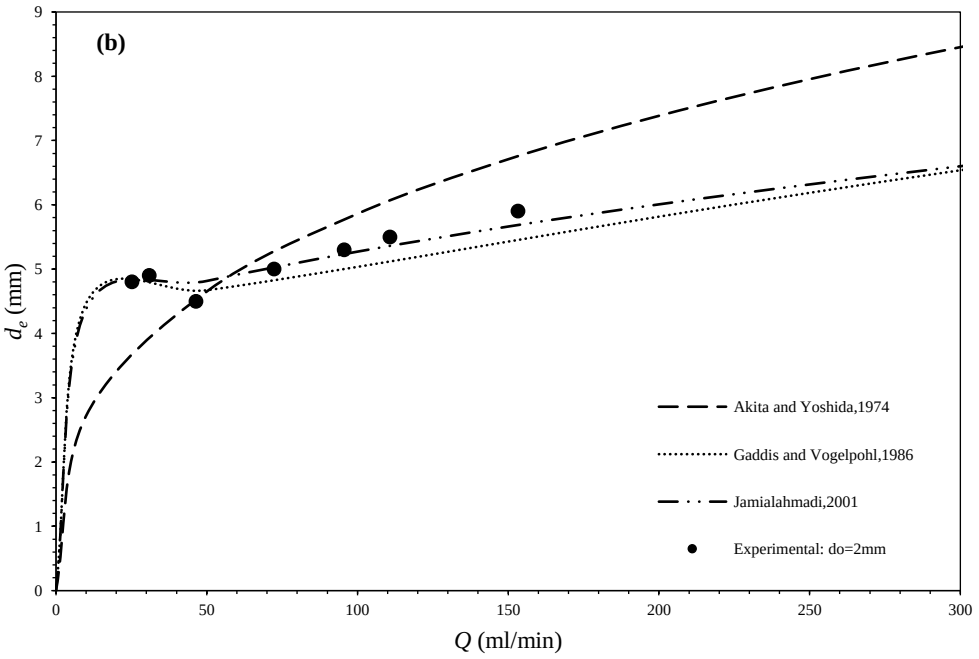
(b)
d_e (mm)
Q (ml/min)
Akita and Yoshida,1974
Gaddis and Vogelpohl,1986
Jamialahmadi,2001
Experimental: do=2mm

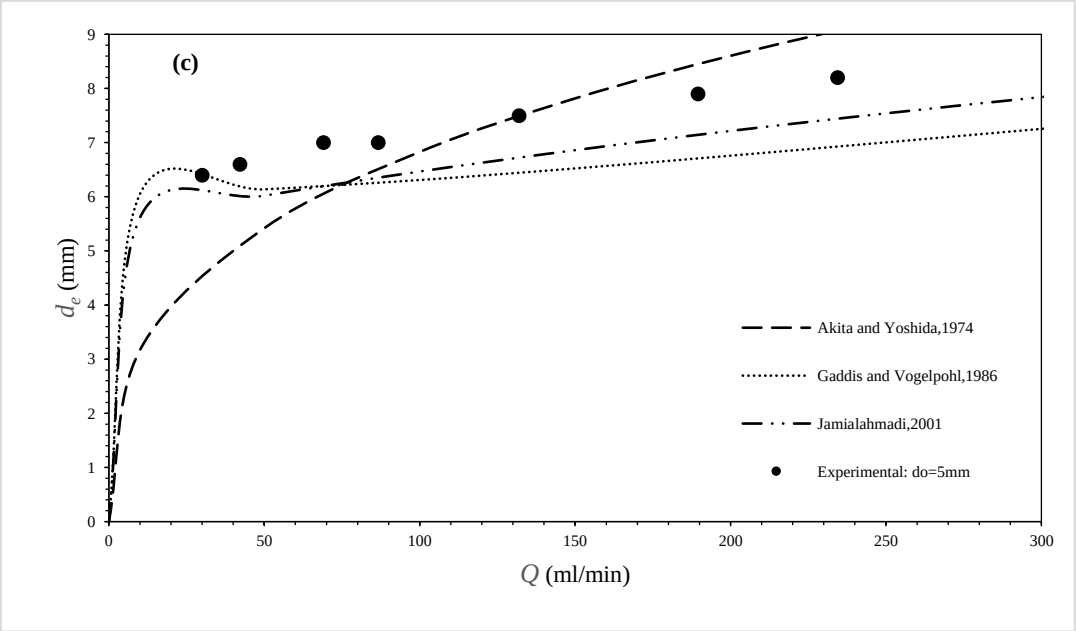

Fig. 6. Comparison *de* versus *Q* between the experimental results and the main authors, for d_o = 1 mm (a), d_o = 2 mm (b) and d_o = 5 mm (c).

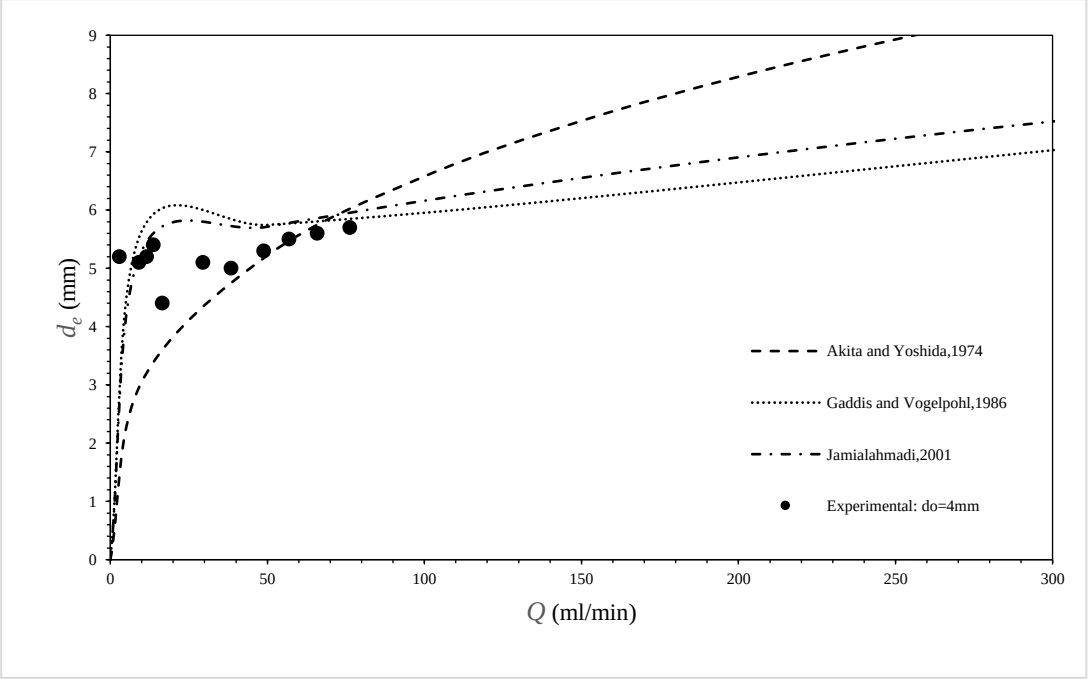

Fig. 7. Comparison *de* versus *Q* between the experimental results from Wang and Socolofsky (2015) and the main authors.